The Journal of Veterinary Medical Science

FULL PAPER

Laboratory Animal Science

Mitotic spindle positioning protein (MISP) deficiency exacerbates dextran sulfate sodium (DSS)-induced colitis in mice

Koki HIURA[1)], Takumi MARUYAMA[1,2)], Masaki WATANABE[1)], Kenta NAKANO[2)], Tadashi OKAMURA[2)], Hayato SASAKI[1)]*, Nobuya SASAKI[1)]*

[1)]Laboratory of Laboratory Animal Science and Medicine, School of Veterinary Medicine, Kitasato University, Aomori, Japan

[2)]Department of Laboratory Animal Medicine, Research Institute, National Center for Global Health and Medicine, Tokyo, Japan

ABSTRACT. Inflammatory bowel disease (IBD) is classified into two types: Crohn's disease and ulcerative colitis. In IBD, the imbalance between the pro-inflammatory and anti-inflammatory cytokines prevents recovery from the inflammatory state, resulting in chronic inflammation in the colon. The mitotic spindle positioning protein (MISP) is localized to the apical membrane in the colon. In this study, we observed increased expression of MISP in the intestinal epithelial cells in dextran sulfate sodium (DSS)-induced colitis in mice. MISP-deficient mice receiving DSS showed significant exacerbation of colitis (e.g., weight loss, loss of the crypts). The intestinal epithelial cells of the MISP-deficient mice showed a trend towards decreased cell proliferation after DSS treatment. Reverse transcription followed by quantitative polymerase chain reaction revealed that the expression levels of *Tgfb1*, an anti-inflammatory cytokine, were significantly reduced in the colon of MISP-deficient mice compared with the wild-type mice regardless of DSS treatment. These findings indicate that MISP may play a role in the recovery of the colon after inflammation through its anti-inflammatory and proliferative activities, suggesting that MISP may be a new therapeutic target for IBD.

KEYWORDS: dextran sulfate sodium-induced colitis, inflammatory bowel disease, inflammatory cytokines, mitotic spindle positioning protein

J. Vet. Med. Sci.
85(2): 167–174, 2023
doi: 10.1292/jvms.22-0483

Received: 25 October 2022
Accepted: 7 December 2022
Advanced Epub:
30 December 2022

Inflammatory bowel disease (IBD) is an intractable bowel disease classified into two types: Crohn's disease (CD) and ulcerative colitis (UC). CD can affect any part of the intestine (primarily the ileum and colon), and the affected area is diffuse. On the other hand, UC only affects the colon (initially the rectum), and the affected area is not diffuse. The clinical symptoms of CD are chronic diarrhea, weight loss, fatigue, and anorexia; those of UC are bloody stools and diarrhea [1, 31, 34]. Inflammation of the intestinal mucosa has been reported to greatly increase the risk of inflammatory carcinogenesis [8]. Although the causes of IBD are poor understood, a population-based study has suggested that the two forms of IBD have common genetic predispositions and triggers [3]. Genome-wide association studies (GWASs) have identified several IBD-associated genes, such as HLA class II histocompatibility antigen, DR alpha chain (*HLA-DR*) [27], Janus kinase 2 (*JAK2*), signal transducer and activator of transcription 3 (*STAT3*) [33], interleukin 10 (*IL-10*), Fc gamma receptor IIa (*FCGR2A*), and solute carrier family 26 member 3 (*SLC26A3*) [2]. Furthermore, recent GWASs have identified and validated approximately 200 loci associated with IBD, with the majority being shared by CD and UC [29, 36]. High-density genotyping, targeted sequencing studies, whole-exome sequencing and whole genome sequencing studies have identified the approximately 20 causal genes. Importantly, these studies have revealed key biological functions in the pathogenesis of IBD, including microbial recognition, autophagy, cytokine signaling, and intestinal epithelial barrier function [28].

Mitotic spindle positioning protein (MISP) is an actin-bundling protein with multiple actin-binding sites [19]. Early studies reported that MISP plays roles in both mitotic progression and spindle positioning [22, 39]. According to the Human Protein Atlas (http://www.proteinatlas.org), MISP is predominantly expressed in the intestinal apical membrane [32]. Morales *et al*. confirmed this in mice and showed that MISP was highly localized to the microvillar rootlets at the brush border. They also showed that MISP stabilizes and elongates the rootlet end of the core actin bundles of the microvillus [25]. Thus, MISP might contribute to the maintenance of the intestinal mucosa or to the pathogenesis of IBD. However, the role of MISP in preclinical models of colitis has not been reported. In

*Correspondence to: Sasaki H: hsasaki@vmas.kitasato-u.ac.jp; Sasaki N: nobsasa@vmas.kitasato-u.ac.jp, Laboratory of Laboratory Animal Science and Medicine, School of Veterinary Medicine, Kitasato University, 35-1 Higashi-23, Towada, Aomori 034-8628, Japan

this study, we generated *Misp* knockout (KO) mice. *Misp* KO mice were healthy and exhibited no histological abnormalities in the intestines. Furthermore, we used the DSS colitis model, which is very popular in IBD research, to determine the contribution of MISP to pathological intestinal inflammation. *Mis*p KO mice showed more severe symptoms than wild-type (WT) controls.

MATERIALS AND METHODS

Ethical statement

All animal experiments complied with the ARRIVE guidelines and were performed in accordance with the Act on Welfare and Management of Animals in Japan. The research was conducted according to the Regulations for the Care and Use of Laboratory Animals of Kitasato University. Animal experimentation protocol was approved by the President of Kitasato University through the judgment by Institutional Animal Care and Use Committee of Kitasato University (Approval ID: 20-039). A humane endpoint was applied when the mice were moribund by 20% weight loss or severe anemia.

Animals

Misp KO mice were generated by CRISPR/Cas9-mediated genome editing [21]. The crRNA sequence was designed to target the mouse *Misp* gene on exon 2 (NCBI accession number: NM_030218.2) as follows: 5′-UUCCUUCAUUGGUGACGUGAGUUUUAGAGCUAUGCUGUUUUG-3′. The crRNA and tracrRNA were artificially synthesized (Fasmac, Tokyo, Japan). The recombinant Cas9 protein (60 ng/mL, New England Biolabs, MA, USA), crRNA (0.61 pmol/mL), and tracrRNA (0.61 pmol/mL) were introduced into fertilized eggs of FVB/NJcl mice (purchased from CLEA Japan, Tokyo, Japan) by microinjection. Two-cell stage embryos were implanted into pseudopregnant mice, and the pups were obtained. The introduction of the null mutation was detected by DNA sequencing using the following primers: forward, 5′-GAACCCCACCAGGCATCAA-3′; reverse, 5′-GGATTCTGCCTGGGTCTGAC-3′. The resulting founder mice were backcrossed to FVB/NJcl mice for three generations. The heterozygous mice were crossed to produce homozygous mice. Animal facilities were air-conditioned, and the mice were maintained at 22 ± 2°C with 40–60% relative humidity under a 12-hr light/dark cycle. Standard laboratory feed CE-2 (CLEA Japan) and tap water were provided *ad libitum*.

DSS-induced colitis

Colitis was induced in 8-week-old male WT and *Misp* KO mice (n=4 per group) by treatment with 3% (w/v) DSS (36,000–50,000 Da; MP Biomedicals, Santa Ana, CA, USA) supplied in drinking water for 5 days. Two days after suspending DSS administration (day 7), all mice were euthanized with inhalation of an overdose of isoflurane. Colitis symptoms were evaluated daily using the disease activity index (DAI), a method of assessing DSS enteritis symptoms (Table 1) [7, 12]. Three scores consisting of the rate of weight loss, stool characteristics, and intensity of bloody stools were summed to evaluate colitis. Similar pathological changes have been observed in the proximal and distal colon after DSS treatment, although less local inflammation has been reported in the proximal colon [23]. In this study, the colon was divided into three sections (proximal, middle, and distal colon) for molecular biological analysis and histological changes from the one mouse; the proximal colon was used for RT-qPCR, the middle colon for Western blot analysis, and the distal colon for histopathological analysis.

Histopathological analysis

The collected distal colon samples were fixed in 10% formalin overnight at 4°C and embedded in paraffin. Paraffin-embedded samples were sectioned at 3 µm thickness and stained with hematoxylin and eosin (HE). HE-stained sections were imaged by light microscopy. The length of the muscularis mucosa was measured by ImageJ software and used as a reference for tissue fragment length. The length of the remaining intramucosal crypt was measured and the crypt loss rate (%) was calculated. These measurements were performed using ImageJ software [30].

Immunofluorescent (IF) staining

The paraffin-embedded colon was sectioned at 5 µm thickness. Antigen retrieval was performed by incubation for 45 min at 98°C in an antigen retrieval reagent (Immunosaver; Nissin EM, Tokyo, Japan). For blocking nonspecific binding, the sections were incubated with 5% goat serum and 0.1% Triton X in phosphate buffered-saline (PBS) for 1 hr at room temperature. After blocking, the sections were incubated with rabbit polyclonal anti-MISP antibody (1:100, 26338-1-AP; Proteintech, Rosemont, IL, USA) at 4°C overnight. Next, the sections were incubated with Alexa Fluor 488-conjugated goat anti-rabbit IgG secondary antibody (1:1,000, A11034; Cell Signaling Technology, Danvers, MA, USA) for 30 min at room temperature. Sections were mounted with ProLong Diamond Antifade Mountant with DAPI (Thermo Fisher Scientific, Waltham, MA, USA). The samples were imaged using an LSM 710 confocal microscope (Carl Zeiss, Oberkochen, Germany).

Table 1. Disease activity index (DAI) score

Score	Body weight loss (%)	Stool consistency	Bleeding
0	1 >	Normal	No bleeding
1	1–5		
2	5–10	Loose stools	Slightly bleeding
3	10–15		
4	15 <	Diarrhea	Gross bleeding

Immunohistochemical (IHC) analysis

Preparation of sections from paraffin-embedded samples and antigen retrieval were performed in the same process above-mentioned. To inactivate endogenous peroxidase, the section was incubated with 3% hydrogen peroxide (H_2O_2) for 30 min. After

blocking for 30 min with 10% normal goat serum, the section was incubated with rabbit polyclonal anti-MISP antibody (1:250, 26338-1-AP) or rabbit monoclonal anti-Ki-67 antibody (418071, Nichirei Biosciences, Tokyo, Japan) overnight at 4°C. Sections were reacted with peroxidase-conjugated anti-rabbit IgG polyclonal antibody (418261, Nichirei Bioscience) for 30 min, and stained with 3,3-diaminobenzidine (DAB; 040-27001, Wako, Tokyo, Japan). The intensity of DAB staining was measured with ImageJ software, and the percentage of positive cells was calculated.

Western blot analysis

Colon tissues from WT mice induced colitis and from 9-week-old WT and *Misp* KO mice treated with tap water were collected and lysed with RIPA buffer. Samples were thermally denatured with 2% sodium dodecyl sulfate (SDS) and 5% 2-mercaptoethanol, electrophoresed on SDS-polyacrylamide gels, and transferred to hydrophobic polyvinylidene fluoride membranes (PALL, Port Washington, NY, USA). In order to block non-specific binding, the membranes were incubated in Bullet Blocking (Nacalai Tesque, Kyoto, Japan) for 5 min at room temperature. Membranes were incubated with rabbit polyclonal antibody against MISP (1:1,000, 26338-1-AP) or mouse monoclonal antibody against GAPDH (1:5,000, HRP-60004, Proteintech) at 4°C overnight. Thereafter, the membranes were incubated with horseradish peroxidase (HRP)-conjugated goat antibody against rabbit IgG (1:1,000, #7074, Cell Signaling) for 1 hr at room temperature. After incubation of the membrane with ECL prime Western Blotting Detection Reagents (Cytiva, Marlborough, MA, USA), imaging was performed using an Omega Lum C imaging system (Gel Co., San Francisco, CA, USA).

RNA extraction and RT-qPCR

RNA was extracted from the proximal colon using TRI reagent (Molecular Research Center, Cincinnati, OH, USA). cDNA synthesis by reverse transcription of the extracted RNA was performed using ReverTra Ace (TOYOBO, Osaka, Japan). Quantitative PCR (qPCR) was performed using THUNDERBIRD® SYBR qPCR Mix (TOYOBO) and the Eco Real-Time PCR system (Illumina, Wilmington, MA, USA). The PCR primer sequences are shown in Table 2.

Statistical analysis

Data are expressed as the means ± standard deviation. Welch's *t*-test was used to analyze differences in body weight change rate, crypt damage rate, and western blot analysis results between the two groups. Mann-Whitney *U* test was used to analyze differences in DAI scores between two groups. Conover Iman test was used to analyze differences in mRNA expression levels, and immunohistochemical results among multiple groups. A *P* value smaller than 0.05 was considered to indicate a statistically significant difference. All statistical analyses were performed using Python (v3.8).

RESULTS

MISP expression in a mouse model of colitis

We investigated the expression of MISP in DSS-induced colitis model. Consistent with previous reports [25, 32], IF and IHC staining showed that MISP was expressed predominantly in the apical membrane of the colon in WT mice after vehicle or DSS treatment (Fig. 1A, 1B). The staining intensities of MISP in the intestinal crypt cells in DSS-treated WT mice were significantly higher than those in control WT mice (Fig. 1C). Consistently, western blot analysis revealed a significant upregulation of MISP expression in the colon samples from WT mice treated with DSS (Fig. 1D, 1E).

Production of MISP-deficient mice with CRISPR/Cas9 system

We generated the *Misp* KO mice carrying a 5-base deletion in exon 2 of *Misp* using a CRISPR/Cas9 system. This deletion leads to frame-shift mutations and pre-mature stop codon (Fig. 2A). Western blot analysis confirmed the ablation of MISP expression in the colon from *Misp* KO mice (Fig. 2B). *Misp* KO mice were healthy and exhibited no histological abnormalities in intestines (Fig. 2C).

Misp KO mice subjected to DSS-induced colitis

To investigate the functional role of MISP in colitis, we subjected *Misp* KO mice to DSS-induced colitis. DSS-treated WT mice showed no significant weight loss, while DSS-treated *Misp* KO mice exhibited marked weight loss starting on day 5, resulting in a

Table 2. Sequences of primers used for RT-qPCR

Gene name	Forward primer	Reverse primer	Accession No.	Product size (bp)
Gapdh	5′-CGACTTCAACAGCAACTC-3′	5′-GCCGTATTCATTGTCATACCAG-3′	NM_001289726.1	106
Il-1b	5′-TGGGCCTCAAAGGAAAGAAT-3′	5′-CAGGCTTGTGCTCTGCTTGT-3′	NM_008361.4	216
Il-6	5′-ACAACCACGGCCTTCCCTACTT-3′	5′-CACGATTTCCCAGAGAACATGTG-3′	NM_031168.2	129
Tnfa	5′-ACCCTCACACTCAGATCATCTTC-3′	5′-TGGTGGTTTGCTACGACGT-3′	NM_013693.3	71
Il-10	5′-TTTCTCCCCTGTGAAAATAAGAGCA-3′	5′-GACACCTTGGTCTTGGAGCTTATTA-3′	NM_010548.2	78
Tgfb1	5′-TGCTTCAGCTCCACAGAGAA-3′	5′-TGGTTGTAGAGGGCAAGGAC-3′	NM_011577.2	182
Wnt5a	5′-CATGTCTTCCAAGTTCTTCCTAATG-3′	5′-GATACAAGTGGCAGAGTTTCTTCTG-3′	NM_009524.4	200

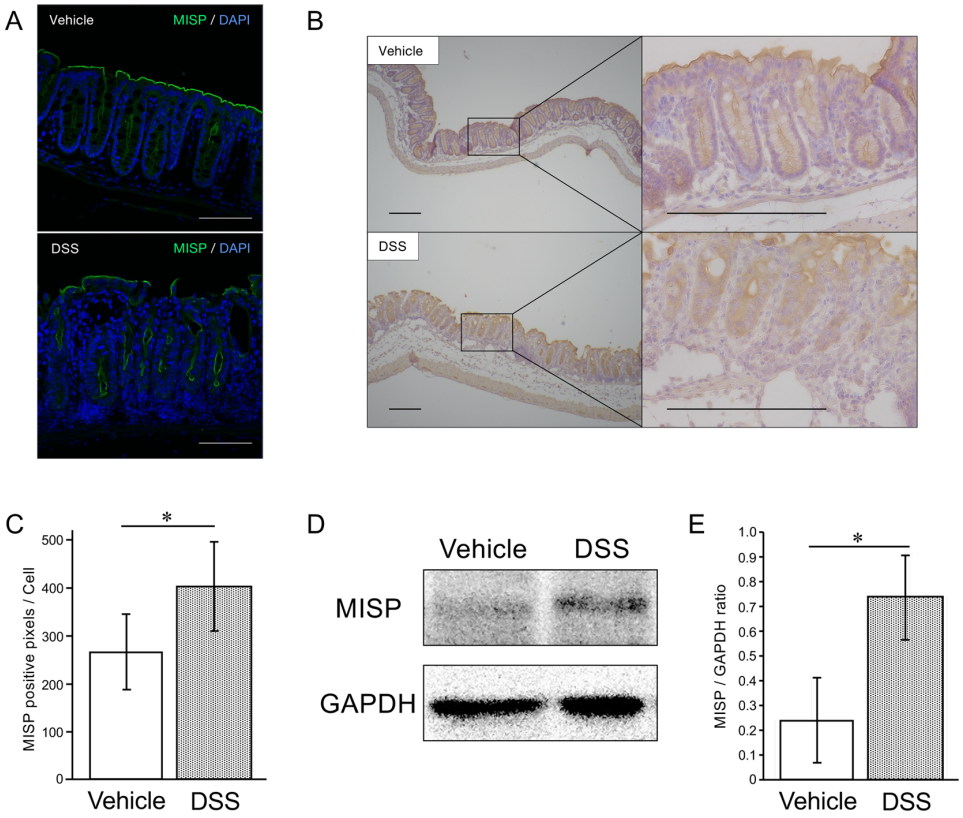

Fig. 1. Alteration of mitotic spindle positioning protein (MISP) expression in a dextran sulfate sodium (DSS)-induced colitis model. (A, B) Representative images of immunofluorescent (IF) (**A**) and Immunohistochemical (IHC) (**B**) staining for MISP with distal colon samples from mice treated with vehicle or DSS (A: Scale bars, 100 µm, B: Scale bars, 200 µm). (**C**) Comparison of 3,3-diaminobenzidine (DAB) staining in IHC staining for MISP in intestinal colon samples treated with vehicle or DSS (n=3 [vehicle group] and 4 [DSS group]; *, $P<0.05$). (**D**, **E**) Comparison of MISP expression levels in mid colon samples treated with vehicle or DSS by western blot analysis (n=3 per group; *, $P<0.05$).

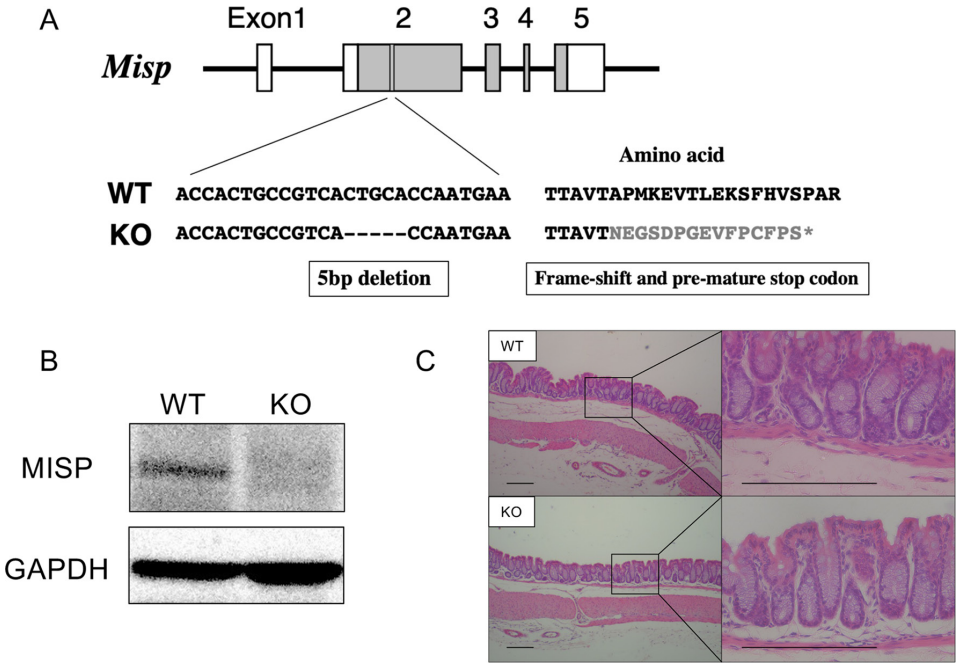

Fig. 2. Generation of mitotic spindle positioning protein (*Misp*) knockout (KO) mice using the CRISPR/Cas9 System. (**A**) Gene structure diagram of *Misp*. The boxes indicate the exons, and the lines connecting boxes are the introns. Grey areas in the boxes indicate coding regions, and white areas in the boxes indicate noncoding regions. KO mice have 5 bp deletion in the exon 2, which might lead to frame-shift mutations and pre-mature stop codon (described as gray font). (**B**) Western blot analysis confirming the MISP deletion in *Misp* KO mice. (**C**) Representative images of colon tissues from wild-type (WT) and *Misp* KO mice. Scale bars, 200 µm.

17.5% weight loss on day 7 (Fig. 3A). DSS-treated *Misp* KO mice also started to show loose stools, diarrhea, and bloody stools on day 6. Accordingly, DSS-treated *Misp* KO mice showed a significant increase in DAI scores after day 5. In contrast, DSS-treated WT mice showed no severe clinical symptoms and, consequently, their DAI scores remained almost at normal levels throughout the observation period (Fig. 3B). The extent of histological damage in colon tissues was strikingly different between the two groups. In DSS-treated WT mice, ulcers were partially observed with inflammatory cell infiltration and structural disruption of the crypts only in the ulcer area. In *Misp* KO mice treated with DSS, extensive pathological changes were observed, including goblet cell reduction and diffuse ulcers. In addition, *Misp* KO mice showed a complete loss of crypts in a wide area of the distal colon compared with WT mice (Fig. 3C). The mean ratio of crypt loss in the *Misp* KO mice was 65.1%, significantly elevated compared with the 33.4% loss seen in the WT mice (Fig. 3D). To investigate the cause of this difference in crypt loss, we first evaluated cell proliferation in the crypts by IHC. Ki-67 positive cells were found in the crypts, and DSS exposure significantly increased Ki-67-positive cells in WT and *Misp* KO mice. There was no difference in the abundance of Ki-67 positive cells between WT and *Misp* KO mice receiving tap water. However, among the DSS-treated mice, there was a trend of decrease in Ki-67-positive cells in *Misp* KO mice compared with WT mice (Fig. 3E, 3F).

Effect of MISP deficiency on pro- and anti- inflammatory cytokines and tissue repair in DSS-induced colitis model

Next, we examined the expression levels of pro-inflammatory and anti-inflammatory cytokines, *Il-1b*, *Il-6*, *Tnfa*, *Il-10*, and *Tgfb1*, in the colon. Transcript levels of *Il-1b*, *Il-6*, and *Tnfa* were highly elevated in mice treated with DSS regardless of the presence of MISP (Fig. 4A–C). In contrast, the level of *Il-10* was unaffected and the level of *Tgfb1* was downregulated, respectively, upon DSS treatment in WT mice. MISP-deficient mice exhibited reduced levels of *Il-10* and *Tgfb1*, and consequently no further downregulation of *Il-10* in response to DSS treatment. The expression levels of *Tgfb1* in *Misp* KO mice were significantly lower than those in DSS-treated WT mice (Fig. 4D, 4E). The TGF-β pathway has been shown to promote crypt budding in wound epithelium in synergy with WNT5A [24]. Therefore, we examined the expression level of *Wnt5a* in the colon. Interestingly, in vehicle treated animals, MISP-deficient mice showed a significant decrease of *Wnt5a* compared to WT mice, however, there is no significant difference between groups in DSS treated animals (Fig. 4F).

DISCUSSION

In the present research, we examined the function of MISP in colitis using a mouse model of DSS-induced colitis. We first examined the changes in the localization and expression levels MISP upon DSS treatment in mice. In vehicle or DSS treated animals, MISP expression was observed in the apical membrane. In addition, MISP expression in the colon was significantly elevated in DSS-treated animals. In *Misp* KO mice receiving tap water, no obvious symptoms were detected. Colitis induction by DSS exposure resulted in significant increases in weight loss and DAI scores in *Misp* KO mice compared with the WT mice. Moreover, extensive crypt loss was noted in *Misp* KO mice relative to the WT mice. Our results indicate that MISP is upregulated in response to colitis and helps in the preservation of colon homeostasis. Accordingly, MISP deficiency exacerbates colitis.

PLK1 regulates mitosis by phosphorylating downstream targets [6]. Decreased expression of PLK1 causes disruption of the balance between proliferation and apoptosis of intestinal epithelial cells in sepsis, leading to an impairment of the barrier function of the intestinal mucosa [4]. MISP is a substrate of PLK1 and is required for correct mitotic spindle positioning. Knockdown of MISP in Hela cells interferes with mitosis by causing spindle misorientation and spindle activity checkpoint-dependent delay in metaphase-to-anaphase transition [39]. To examine whether MISP deficiency exacerbates intestinal tissue damage by delaying tissue repair, we evaluated the expression of Ki-67, a marker of cell proliferation. The results suggest that cell proliferation in the crypts is reduced in *Misp* KO mice compared with the WT mice.

Intestinal stem cells are located at the base of the crypts and function to repair the mucosal layer after injury by continuously regenerating the mucosa to maintain normal intestinal homeostasis. Dysfunction of intestinal stem cells disrupts the mucosal barrier, allowing luminal contents to invade the mucosa [10, 11, 37]. DSS treatment is thought to induce damage to the barrier function of the intestinal mucosa [5], and *Misp* KO mice show a tendency to suppress colon stem cell proliferation, suggesting that they may have been more significantly affected by the DSS-induced damage compared with the WT mice. MISP also binds to actin filaments in the cytoplasm and localizes to the plasma membrane, suggesting that it is involved in the formation of the cytoskeleton [39]. In the colon, MISP is expressed on the apical membrane of colonic epithelial cells, suggesting that MISP deficiency itself may affect the barrier function of the colonic mucosa.

In IBD, an imbalance between pro-inflammatory and anti-inflammatory cytokines has been reported to inhibit the convergence of inflammation causing prolonged disease and tissue damage [26]. Therefore, we examined mRNA expression levels of cytokines in the colon. The cytokines measured were indicators of Th2 (*Il-10*), Treg (*Il-10*, *Tgfb1*), and Th17 (*Il-6*, *Tgfb1*) cells, and of innate immune responses (*Il-1b*, *Tnfa*) [38]. The expression of the inflammatory cytokines *Il-1b*, *Il-6*, and *Tnfa* increased by DSS treatment, suggesting that the inflammation in the colon caused by DSS treatment is reflected in the mRNA expression levels. However, no differences were detected in the expression levels of these cytokines between WT and *Misp* KO mice treated with DSS. Accordingly, our results suggest that inflammatory cytokines are not responsible for the malignant transformation of DSS-induced colitis caused by MISP deficiency.

The anti-inflammatory cytokines IL-10 and TGF-β are produced by Treg cells and are protective against colitis [15, 16]. Treg cells have been found to be decreased in the peripheral blood of IBD patients [9]. In several IBD models, transplantation of Treg cells has been found to control inflammatory lesions. It has been reported that alterations in the balance between $Foxp3^+$ $CD4^+$ Treg cells and T effector cells in the intestinal microenvironment contribute to the pathogenesis of IBD [35]. Pancreatic ductal adenocarcinoma tissues with high MISP expression show significantly increased infiltration of follicular helper T cells, Treg, activated natural killer

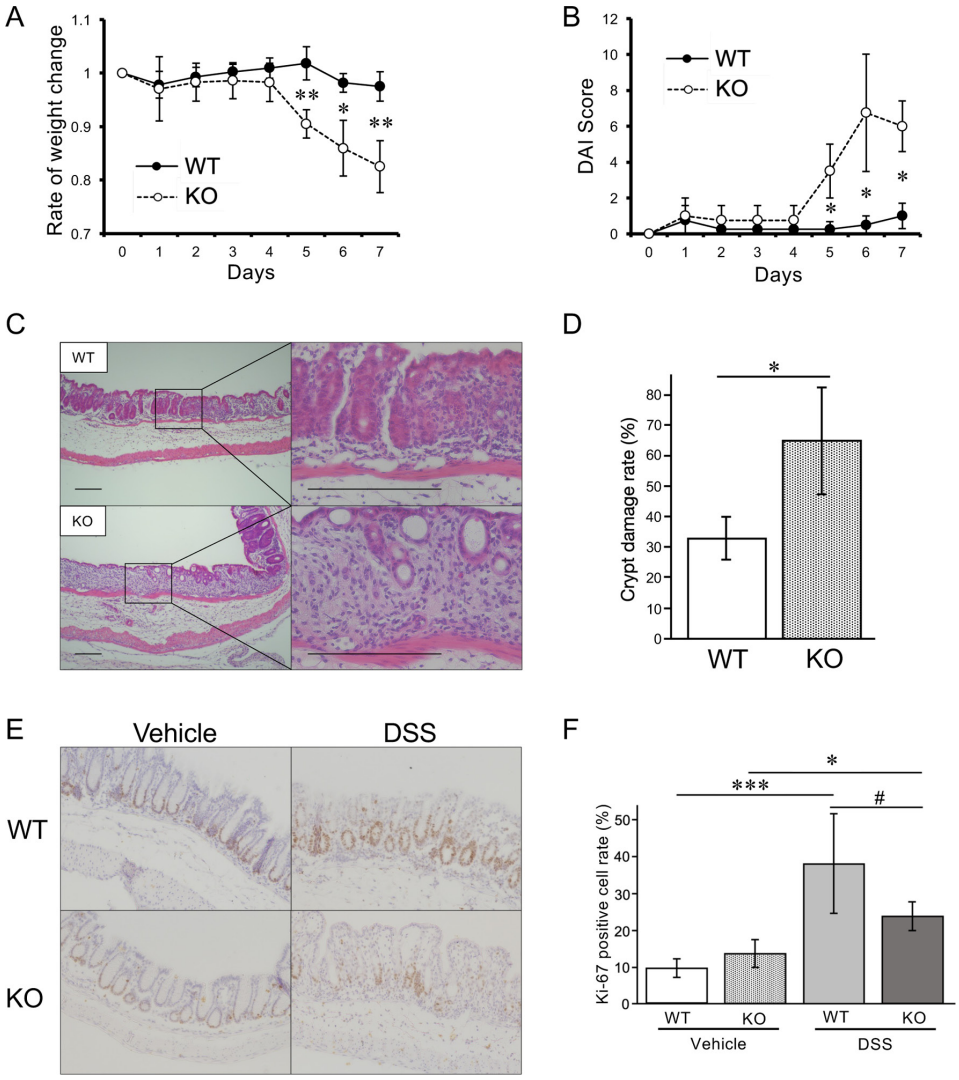

Fig. 3. Effect of mitotic spindle positioning protein (MISP) deficiency in mice with dextran sulfate sodium (DSS)-induced colitis. (A, B) Comparison of body weight changes (**A**) and disease activity index (DAI) scores (**B**) in wild-type (WT) and *Misp* knockout (KO) mice in DSS-induced colitis model (n=4 per group; *, $P<0.05$; **, $P<0.01$). (**C**) Representative pathology images of the colon samples from WT and *Misp* KO mice treated with DSS. Scale bars, 200 µm. (**D**) Comparison of the rates of crypt damage in the colon samples from WT and *Misp* KO mice treated with DSS (n=4 per group; *, $P<0.05$). (E, F) Representative images of Immunohistochemical (IHC) staining for Ki-67 (**E**) and comparison of the rates of Ki-67 positive cells in WT and *Misp* KO mice treated with vehicle or DSS (**F**) (n=3 per group of vehicle-treated mice; n=4 per group of DSS-treated mice; #, $P<0.1$; *, $P<0.05$; ***, $P<0.001$). Scale bars, 200 µm.

(NK) cells, and M0 macrophages, and decreased infiltration of activated $CD4^+$ memory T cells, CD8+ T cells, resting NK cells, monocytes, M2 macrophages and neutrophils. This suggests that MISP has a specific role in limiting and inhibiting T cell activation. [14]. The expression levels of *Il-10* and *Tgfb1* were significantly reduced in *Misp* KO mice compared with WT mice treated with vehicle (control groups), and the expression levels of *Tgfb1* in *Misp* KO mice were also lower than those in WT mice receiving DSS (colitis groups). These results suggest that MISP expression might be involved in Treg infiltration. IL-10 receptor and its downstream signaling pathways are thought to play critical roles in regulating intestinal homeostasis and immunity. Polymorphisms in these genes in innate immune cells have been linked to dysregulation of mucosal immune tolerance and early onset of IBD [27]. IL-10 is recognized by macrophages and alleviates DSS-induced colitis by suppressing the production of nitric oxide and reactive oxygen species [20]. IL-10 KO mice exhibit spontaneous colitis development, resulting in anemia and growth retardation [17]. The reduced levels of *Il-10* expression in *Misp* KO mice in the absence of DSS treatment suggest that it potentially increases susceptibility to DSS-induced colitis.

The TGF-β family consists of five different isoforms (TGF-β1 to β5), which suppress cytokine production by inhibiting macrophage and Th1 cell activity [38]. TGF-β1-deficient mice show inflammatory phenotypes in multiple organs, including the colon, within weeks of birth [18]. However, the low levels of *Tgfb1* expression in *Misp* KO mice had no effect on the expression of pro-inflammatory cytokines in the colitis model in this study. Loss of TGF-β signaling in the intestine increases susceptibility to ulcerative colitis, suggesting that TGF-β signaling is an important determinant of tissue injury in inflammatory diseases [13]. This is consistent with the significantly decreased levels of *Tgfb1* in the colon of *Misp* KO mice, which exhibited severe symptoms in response to DSS-

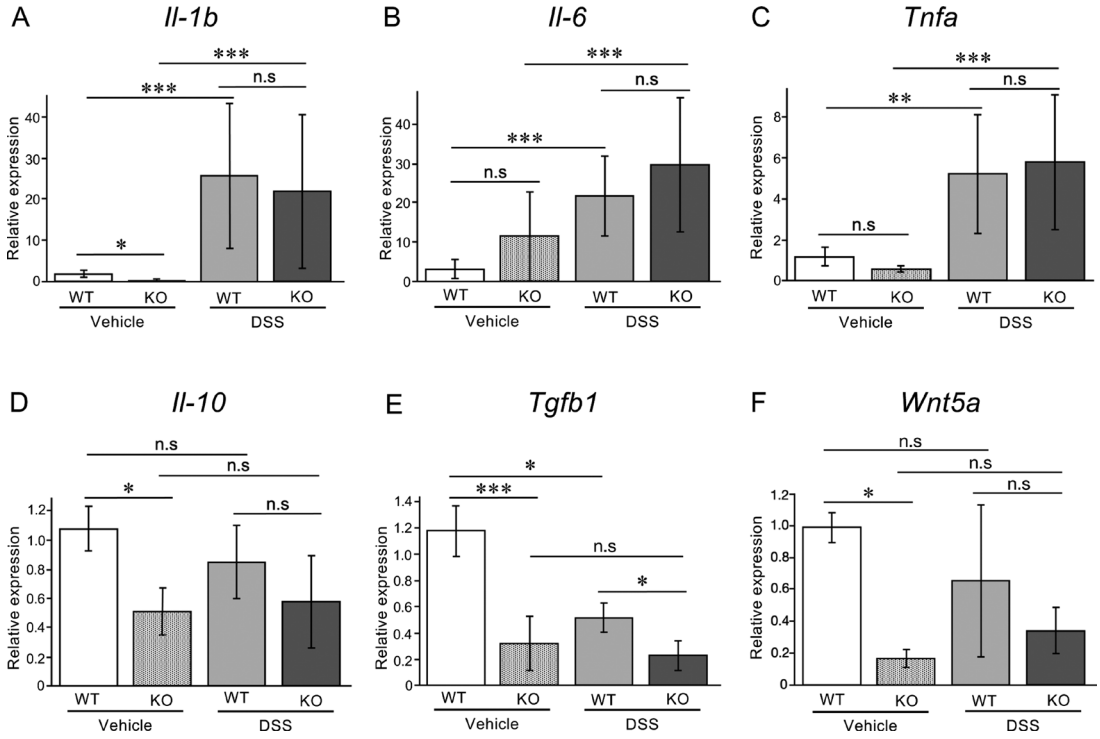

Fig. 4. Effect of mitotic spindle positioning protein (MISP) deficiency on pro- and anti-inflammatory cytokines and tissue repair in dextran sulfate sodium (DSS)-induced colitis model. (A–E) Messenger RNA levels of pro-inflammatory cytokines *Il-1b* (**A**), *Il-6* (**B**), and *Tnfa* (**C**); and anti-inflammatory cytokines *Il-10* (**D**) and *Tgfb1* (**E**); and *Wnt5a* (**F**) in wild-type (WT) and *Misp* knockout (KO) mice with and without DSS-induced colitis (n=3–4 per group; *, $P<0.05$; **, $P<0.01$; ***, $P<0.001$).

mediated colitis induction, and with the increased expression of MISP in WT mice upon DSS treatment. It has also been shown that regeneration of lost crypts requires WNT5A signaling, one of the non-classical Wnt signaling pathways, and that WNT5A promotes crypt regeneration in the repair of colonic injury by activating the TGF-β pathway [24]. Interestingly, *Wnt5a* expression was also decreased in *Misp* KO mice upon vehicle treatment, suggesting a potential loss of tissue repair capacity. The decreased expression of *Tgfb1* in *Misp* KO mice upon DSS treatment may have decreased TGF-β pathway-dependent WNT5A-mediated colonic crypt repair and exacerbated crypt loss.

In conclusion, MISP acts in the repair of damaged crypts in the colon, and its loss suppresses the repair of colonic epithelial damage caused by DSS treatment, resulting in aggravation of colitis. MISP exhibited a protective effect against colitis by regulating the expression of anti-inflammatory cytokines (*Il-10*, *Tgfb1*) but not inflammatory cytokines (*Il-6*, *Il-1b*, *Tnfa*), and promoting tissue repair by regulating WNT5A expression. These findings may facilitate the development of therapies targeting the imbalance between pro-inflammatory and anti-inflammatory cytokines and tissue damage in IBD.

CONFLICT OF INTEREST. The authors have no conflicts of interest directly relevant to the content of this article.

ACKNOWLEDGMENTS. This work was supported by the Ministry of Education, Culture, Sports, Science and Technology (MEXT), Glant-in-Aid for Scientific Research, KAKENHI (22J13213) to KH, KAKENHI (16K16606) to HS and KAKENHI (20302614) to NS. This study was partially supported by the National Center for Global Health and Medicine (20A1019).

REFERENCES

1. Abraham C, Cho JH. 2009. Inflammatory bowel disease. *N Engl J Med* **361**: 2066–2078. [Medline] [CrossRef]
2. Asano K, Matsushita T, Umeno J, Hosono N, Takahashi A, Kawaguchi T, Matsumoto T, Matsui T, Kakuta Y, Kinouchi Y, Shimosegawa T, Hosokawa M, Arimura Y, Shinomura Y, Kiyohara Y, Tsunoda T, Kamatani N, Iida M, Nakamura Y, Kubo M. 2009. A genome-wide association study identifies three new susceptibility loci for ulcerative colitis in the Japanese population. *Nat Genet* **41**: 1325–1329. [Medline] [CrossRef]
3. Bernstein CN, Wajda A, Blanchard JF. 2005. The clustering of other chronic inflammatory diseases in inflammatory bowel disease: a population-based study. *Gastroenterology* **129**: 827–836. [Medline] [CrossRef]
4. Cao Y, Chen Q, Wang Z, Yu T, Wu J, Jiang X, Jin X, Lu W. 2018. PLK1 protects against sepsis-induced intestinal barrier dysfunction. *Sci Rep* **8**: 1055. [Medline] [CrossRef]
5. Chassaing B, Aitken JD, Malleshappa M, Vijay-Kumar M. 2014. Dextran sulfate sodium (DSS)-induced colitis in mice. *Curr Protoc Immunol* **104**: 15.25.1–15.25.14. [Medline]
6. Colicino EG, Hehnly H. 2018. Regulating a key mitotic regulator, polo-like kinase 1 (PLK1). *Cytoskeleton (Hoboken)* **75**: 481–494. [Medline] [CrossRef]

7. Cooper HS, Murthy SN, Shah RS, Sedergran DJ. 1993. Clinicopathologic study of dextran sulfate sodium experimental murine colitis. *Lab Invest* **69**: 238–249. [Medline]
8. Eaden JA, Mayberry JF. British Society for Gastroenterology Association of Coloproctology for Great Britain and Ireland. 2002. Guidelines for screening and surveillance of asymptomatic colorectal cancer in patients with inflammatory bowel disease. *Gut* **51** Suppl 5: V10–V12. [Medline] [CrossRef]
9. Eastaff-Leung N, Mabarrack N, Barbour A, Cummins A, Barry S. 2010. Foxp3+ regulatory T cells, Th17 effector cells, and cytokine environment in inflammatory bowel disease. *J Clin Immunol* **30**: 80–89. [Medline] [CrossRef]
10. Fordham RP, Yui S, Hannan NRF, Soendergaard C, Madgwick A, Schweiger PJ, Nielsen OH, Vallier L, Pedersen RA, Nakamura T, Watanabe M, Jensen KB. 2013. Transplantation of expanded fetal intestinal progenitors contributes to colon regeneration after injury. *Cell Stem Cell* **13**: 734–744. [Medline] [CrossRef]
11. Fukuda M, Mizutani T, Mochizuki W, Matsumoto T, Nozaki K, Sakamaki Y, Ichinose S, Okada Y, Tanaka T, Watanabe M, Nakamura T. 2014. Small intestinal stem cell identity is maintained with functional Paneth cells in heterotopically grafted epithelium onto the colon. *Genes Dev* **28**: 1752–1757. [Medline] [CrossRef]
12. Ghia JE, Blennerhassett P, Collins SM. 2008. Impaired parasympathetic function increases susceptibility to inflammatory bowel disease in a mouse model of depression. *J Clin Invest* **118**: 2209–2218. [Medline]
13. Hahm KB, Im YH, Parks TW, Park SH, Markowitz S, Jung HY, Green J, Kim SJ. 2001. Loss of transforming growth factor β signalling in the intestine contributes to tissue injury in inflammatory bowel disease. *Gut* **49**: 190–198. [Medline] [CrossRef]
14. Huang X, Zhao L, Jin Y, Wang Z, Li T, Xu H, Wang Q, Wang L. 2022. Up-regulated MISP is associated with poor prognosis and immune infiltration in pancreatic ductal adenocarcinoma. *Front Oncol* **12**: 827051. [Medline] [CrossRef]
15. Huber S, Gagliani N, Esplugues E, O'Connor W Jr, Huber FJ, Chaudhry A, Kamanaka M, Kobayashi Y, Booth CJ, Rudensky AY, Roncarolo MG, Battaglia M, Flavell RA. 2011. Th17 cells express interleukin-10 receptor and are controlled by Foxp3^{-} and Foxp3+ regulatory CD4+ T cells in an interleukin-10-dependent manner. *Immunity* **34**: 554–565. [Medline] [CrossRef]
16. Ihara S, Hirata Y, Koike K. 2017. TGF-β in inflammatory bowel disease: a key regulator of immune cells, epithelium, and the intestinal microbiota. *J Gastroenterol* **52**: 777–787. [Medline] [CrossRef]
17. Kühn R, Löhler J, Rennick D, Rajewsky K, Müller W. 1993. Interleukin-10-deficient mice develop chronic enterocolitis. *Cell* **75**: 263–274. [Medline] [CrossRef]
18. Kulkarni AB, Huh CG, Becker D, Geiser A, Lyght M, Flanders KC, Roberts AB, Sporn MB, Ward JM, Karlsson S. 1993. Transforming growth factor beta 1 null mutation in mice causes excessive inflammatory response and early death. *Proc Natl Acad Sci USA* **90**: 770–774. [Medline] [CrossRef]
19. Kumeta M, Gilmore JL, Umeshima H, Ishikawa M, Kitajiri S, Horigome T, Kengaku M, Takeyasu K. 2014. Caprice/MISP is a novel F-actin bundling protein critical for actin-based cytoskeletal reorganizations. *Genes Cells* **19**: 338–349. [Medline] [CrossRef]
20. Li B, Alli R, Vogel P, Geiger TL. 2014. IL-10 modulates DSS-induced colitis through a macrophage-ROS-NO axis. *Mucosal Immunol* **7**: 869–878. [Medline] [CrossRef]
21. Li D, Qiu Z, Shao Y, Chen Y, Guan Y, Liu M, Li Y, Gao N, Wang L, Lu X, Zhao Y, Liu M. 2013. Heritable gene targeting in the mouse and rat using a CRISPR-Cas system. *Nat Biotechnol* **31**: 681–683. [Medline] [CrossRef]
22. Maier B, Kirsch M, Anderhub S, Zentgraf H, Krämer A. 2013. The novel actin/focal adhesion-associated protein MISP is involved in mitotic spindle positioning in human cells. *Cell Cycle* **12**: 1457–1471. [Medline] [CrossRef]
23. Melgar S, Karlsson A, Michaëlsson E. 2005. Acute colitis induced by dextran sulfate sodium progresses to chronicity in C57BL/6 but not in BALB/c mice: correlation between symptoms and inflammation. *Am J Physiol Gastrointest Liver Physiol* **288**: G1328–G1338. [Medline] [CrossRef]
24. Miyoshi H, Ajima R, Luo CT, Yamaguchi TP, Stappenbeck TS. 2012. Wnt5a potentiates TGF-β signaling to promote colonic crypt regeneration after tissue injury. *Science* **338**: 108–113. [Medline] [CrossRef]
25. Morales EA, Arnaiz C, Krystofiak ES, Zanic M, Tyska MJ. 2022. Mitotic Spindle Positioning (MISP) is an actin bundler that selectively stabilizes the rootlets of epithelial microvilli. *Cell Rep* **39**: 110692. [Medline] [CrossRef]
26. Neurath MF. 2014. Cytokines in inflammatory bowel disease. *Nat Rev Immunol* **14**: 329–342. [Medline] [CrossRef]
27. Nomura E, Kinouchi Y, Negoro K, Kojima Y, Oomori S, Sugimura M, Hiroki M, Takagi S, Aihara H, Takahashi S, Hiwatashi N, Shimosegawa T. 2004. Mapping of a disease susceptibility locus in chromosome 6p in Japanese patients with ulcerative colitis. *Genes Immun* **5**: 477–483. [Medline] [CrossRef]
28. Ntunzwenimana JC, Boucher G, Paquette J, Gosselin H, Alikashani A, Morin N, Beauchamp C, Thauvette L, Rivard MÈ, Dupuis F, Deschênes S, Foisy S, Latour F, Lavallée G, Daly MJ, Xavier RJ, Charron G, Goyette P, Rioux JD. iGenoMed Consortium. 2021. Functional screen of inflammatory bowel disease genes reveals key epithelial functions. *Genome Med* **13**: 181. [Medline] [CrossRef]
29. Ramos GP, Papadakis KA. 2019. Mechanisms of disease: inflammatory bowel diseases. *Mayo Clin Proc* **94**: 155–165. [Medline] [CrossRef]
30. Schneider CA, Rasband WS, Eliceiri KW. 2012. NIH Image to ImageJ: 25 years of image analysis. *Nat Methods* **9**: 671–675. [Medline] [CrossRef]
31. Torres J, Mehandru S, Colombel JF, Peyrin-Biroulet L. 2017. Crohn's disease. *Lancet* **389**: 1741–1755. [Medline] [CrossRef]
32. Uhlén M, Fagerberg L, Hallström BM, Lindskog C, Oksvold P, Mardinoglu A, Sivertsson Å, Kampf C, Sjöstedt E, Asplund A, Olsson I, Edlund K, Lundberg E, Navani S, Szigyarto CAK, Odeberg J, Djureinovic D, Takanen JO, Hober S, Alm T, Edqvist PH, Berling H, Tegel H, Mulder J, Rockberg J, Nilsson P, Schwenk JM, Hamsten M, von Feilitzen K, Forsberg M, Persson L, Johansson F, Zwahlen M, von Heijne G, Nielsen J, Pontén F. 2015. Proteomics. Tissue-based map of the human proteome. *Science* **347**: 1260419. [Medline] [CrossRef]
33. Umeno J, Asano K, Matsushita T, Matsumoto T, Kiyohara Y, Iida M, Nakamura Y, Kamatani N, Kubo M. 2011. Meta-analysis of published studies identified eight additional common susceptibility loci for Crohn's disease and ulcerative colitis. *Inflamm Bowel Dis* **17**: 2407–2415. [Medline] [CrossRef]
34. Ungaro R, Mehandru S, Allen PB, Peyrin-Biroulet L, Colombel JF. 2017. Ulcerative colitis. *Lancet* **389**: 1756–1770. [Medline] [CrossRef]
35. Yamada A, Arakaki R, Saito M, Tsunematsu T, Kudo Y, Ishimaru N. 2016. Role of regulatory T cell in the pathogenesis of inflammatory bowel disease. *World J Gastroenterol* **22**: 2195–2205. [Medline] [CrossRef]
36. Younis N, Zarif R, Mahfouz R. 2020. Inflammatory bowel disease: between genetics and microbiota. *Mol Biol Rep* **47**: 3053–3063. [Medline] [CrossRef]
37. Yui S, Nakamura T, Sato T, Nemoto Y, Mizutani T, Zheng X, Ichinose S, Nagaishi T, Okamoto R, Tsuchiya K, Clevers H, Watanabe M. 2012. Functional engraftment of colon epithelium expanded in vitro from a single adult Lgr5^{+} stem cell. *Nat Med* **18**: 618–623. [Medline] [CrossRef]
38. Zhang JM, An J. 2007. Cytokines, inflammation, and pain. *Int Anesthesiol Clin* **45**: 27–37. [Medline] [CrossRef]
39. Zhu M, Settele F, Kotak S, Sanchez-Pulido L, Ehret L, Ponting CP, Gönczy P, Hoffmann I. 2013. MISP is a novel Plk1 substrate required for proper spindle orientation and mitotic progression. *J Cell Biol* **200**: 773–787. [Medline] [CrossRef]